Next Materials 12 (2026) 102253

Contents lists available at ScienceDirect

Next Materials

journal homepage: www.sciencedirect.com/journal/next-materials

Research article

Burnt coconut fibre as a sustainable additive for water-based drilling fluids: Rheological, filtration, and physicochemical evaluation

Ifeanyi Oguamah [a,*], Kevin Igwilo [a], Jeffrey Oseh [a,b], Stephen Udeagbara [c]

[a] Department of Petroleum Engineering, Federal University of Technology, Owerri, Nigeria
[b] Institute of Ecosystem Science Borneo, Universiti Putra Malaysia, 9700, Bintulu, Sarawak, Malaysia
[c] Afe Babalola University, Ado-Ekiti, Nigeria

A R T I C L E I N F O

Keywords:
Drilling mud
Rheological properties
Fluid loss control
Bio-additive
Burnt coconut fibre

A B S T R A C T

The development of sustainable drilling-fluid additives is essential for improving performance while reducing environmental impact. This study evaluates burnt coconut fibre (BCF) as a biodegradable bio-additive to enhance rheological properties, filtration control, and pH stability in water-based drilling fluids, in accordance with API standards. Five mud samples were formulated: a conventional NaOH-based control and four with BCF at concentrations of 29–114 g/L. Key properties, including density, plastic viscosity (PV), apparent viscosity (AV), yield point (YP), gel strength, pH, and fluid loss, were measured using standard API procedures. BCF physicochemical characteristics were analyzed via Fourier Transform Infrared Spectroscopy (FTIR), Scanning Electron Microscopy (SEM), and Energy Dispersive X-ray Spectroscopy (EDS). All measurements were performed in triplicate ($n = 3$), with statistical significance assessed using two-tailed Welch's t-test (unequal variance; $p < 0.01$ for key improvements). Results showed statistically significant reductions in PV and AV across BCF-modified samples ($p < 0.01$), with PV decreasing from 31.5 cP (control) to 14.07–11.20 cP at 29–57 g/L BCF, accompanied by a strong YP of 22–24 lb/100 ft^2. Low-to-moderate concentrations (29–57 g/L) yielded the most favorable rheological profile, while higher loadings (86–114 g/L) caused excessive thinning. Gel strength developed progressively and remained stable, supporting effective solids suspension without excessive rigidity. Filtration tests revealed reduced early-stage filtrate invasion and thin, compact filter cakes at optimal concentrations. BCF moderated alkalinity, maintaining pH at favorable levels of ~8.0. FTIR confirmed hydroxyl and carbonyl groups; SEM showed a porous, fibrous microstructure; and EDS indicated high carbon content (82.7 wt%) with trace alkali elements aiding pH modulation. These findings demonstrate that BCF is a cost-effective, bio-based additive that enhances drilling fluid performance at optimal concentrations.

1. Introduction

The drilling operation is a pivotal part of any hydrocarbon exploration and production. Drilling fluids are complex, multicomponent systems comprising base fluids and functional additives, with compositions that vary according to formulation and operational requirements [1]. The different characteristics of a drilling fluid include rheological properties, filtration and lost circulation control, lubrication, and differential sticking tendencies, as well as thermal and microbial inhibition abilities [2,3]. The basic functions of the drilling fluids in a well operation are to remove and suspend cuttings, lubricate the wellbore and fluid pathway, provide buoyancy to the drill string, cool equipment, and clean the wellbore, help in wellbore stabilization by providing the needed hydrostatic pressure, as well as provide assistance during cementing and completion processes. Studies have shown that drilling mud properties are central to the success of drilling operations [4–6], and, like other non-Newtonian fluids, drilling fluids exhibit shear-thinning behavior. These fluids exhibit high viscosity at low shear rates, enabling effective transport and suspension of drill cuttings. Conversely, they showcase low viscosity under high shear rates, facilitating efficient downhole pumping [7,8]. The conditions of the subsurface and downhole portions of the well determine the driller's design of the mud programme. In their study, [9] proposed that, during drilling operations, unfavourable downhole conditions frequently result in degraded drilling performance and can even lead to critical incidents such as blowouts and well collapses. As downhole conditions vary, the

* Corresponding author.
E-mail address: ifeanyi.oguamah@futo.edu.ng (I. Oguamah).

https://doi.org/10.1016/j.nxmate.2026.102253
Received 15 February 2026; Received in revised form 1 May 2026; Accepted 8 May 2026
Available online 13 May 2026
2949-8228/© 2026 The Author(s). Published by Elsevier Ltd. This is an open access article under the CC BY license (http://creativecommons.org/licenses/by/4.0/).

drilling mud programme will also vary to meet subsurface demands. Regardless of bottom-hole conditions, drilling fluids are typically formulated to exhibit sufficient gel strength, optimal viscosity, appropriate mud weight, and effective filtration and sealing properties. These properties ensure that cuttings are adequately suspended in the mud, pump requirements do not exceed the required horsepower, and thief (or lost circulation) zones are adequately sealed off.

The design of drilling fluid is crucial for the success of any drilling operation. While rheology significantly affects drilling fluid performance, pH is equally vital, especially because of the potential presence of acidic formations during drilling [10]. Understanding pH is key to optimizing operational efficiency and lowering costs. The most commonly used pH modifier is caustic soda (NaOH), due to its complete dissociation and quick reaction with hydronium ions compared to other bases like lime (Ca(OH)2) [11].

Recent research indicates that drilling fluids perform optimally in water-based mud within a pH range of 8.0–10.5 [12,13]. Contaminants like chlorides, sulfides, and carbonates, which are commonly found in formations, significantly influence mud properties. These substances are often components of natural gas during drilling and form acids in water, affecting the mud's pH. This can lead to issues such as flocculation, thickening, dispersion, and clay separation. Therefore, continuous monitoring of formation pressure allows for dynamic adjustment of mud weight to ensure optimal hydrostatic pressure, enabling secure drilling through contaminated formations. Furthermore, adverse contaminant-induced effects are minimized by keeping the pH of the water-based drilling fluid in the 10.5–11.5 range [14].

Due to the global release of large volumes of aqueous waste into streams, many oil and gas operators are actively seeking substitutes for highly toxic and environmentally harmful drilling fluid additives. A promising alternative is the use of natural or bio-based additives, which are characterized by low toxicity and high biodegradability [15–17]. In one of the earlier studies in this area, Alkinani et al. [18] evaluated palm tree leaf powder (PTLP) as a rheological and filtration control additive. The study reported moderate improvements in plastic viscosity and yield point, although its performance was somewhat lower than that of conventional starch-based additives. Building on this foundation, Al-Hameedi et al. [19] introduced black sunflower seed shell powder (BSSSP), reporting greater improvements in fluid loss control and rheological behavior, and establishing BSSSP as a viable eco-friendly alternative.

Subsequent works expanded the scope of materials. For instance, Shuvo et al. [20] assessed sawdust and found it moderately effective in reducing fluid loss. However, it produced thick, rough mud cakes, highlighting the importance of optimizing particle morphology. In the same study, rice husk outperformed sawdust in fluid loss reduction (~77%) but lacked supporting rheological data, revealing a recurring gap in comprehensive performance analysis. Seeking more structurally consistent additives, Zhou et al. [21] investigated wild jujube pit powder (WJPP). The results showed that wild jujube pit powder not only enhanced viscosity and shear-thinning behavior but also enhanced compact grid-like mud cake formation. Murtaza et al. [22] took an experimental and modeling approach to determine the suitability of okra as a fluid loss control additive, which, at low concentrations, formed thin, impermeable filter cakes and significantly reduced fluid loss, without negatively impacting rheology.

In a broader comparative study, Oladipo et al. [23] tested biodegradable vegetable peels (pumpkin, courgette, squash) and found that finely ground pumpkin peel (10 μm) produced the most notable results, reducing fluid loss by 43.5%, improving gel strength, and increasing pH to around 10.5. This study reinforced previous findings on particle size dependency and further emphasized the multifunctional potential of certain plant-based materials.

Cellulose-based additives, particularly cellulose nanomaterials, cellulose nanofibers (CNFs), and cellulose nanocrystals (CNCs), have emerged as sustainable enhancers for water-based drilling fluids due to their superior rheological and filtration properties [24]. Their effectiveness depends strongly on structure and surface chemistry, with different CNF types offering distinct advantages in rheology and fluid loss control. However, performance degradation under high-temperature and high-salinity conditions remains a key limitation [25]. Recent studies show that polymer modification significantly improves thermal stability, salt tolerance, and filtration performance by enhancing colloidal stability [26].

These advances highlight the potential of engineered cellulose-based systems for developing robust drilling fluids for extreme environments.

Most recently, Safian et al. [27] explored a more engineered approach using bio-graphene derived from coconut husk, demonstrating improved thermal stability and fluid loss control. This research marks a shift toward value-added conversion of biodegradable lignocellulosic material, thereby combining structural benefits with environmental sustainability.

Across these studies, a consistent trend emerges: the effectiveness of natural additives is influenced not only by their chemical composition but also by their particle size, morphology, and concentration. Recent studies have explored bio-based and fibrous materials as alternative drilling fluid additives; however, their combined physicochemical properties and performance remain insufficiently understood. In particular, the behavior of thermally treated bio-based fibres, such as coconut fibre, has not been systematically investigated, especially in relation to their structural modification and its impact on rheological and filtration performance. Therefore, the core objective of this study is to investigate the potential of burnt coconut fibre (BCF) as a multifunctional additive for water-based drilling fluids by systematically evaluating its physicochemical properties and correlating these with its effects on rheological behavior, filtration performance, and pH stability. From a sustainability viewpoint, this study is in line with the United Nations Sustainable Development Goals, especially SDG 12 (Responsible Consumption and Production), because it encourages the use of agricultural waste as a function drilling fluid additive. Using BCF minimizes the need for synthetic materials and encourages sustainable resource utilization. The development of bio-based additives contributed to SDG 9 (Industry, Innovation and Infrastructure) by advancing environmentally conscious drilling solutions, while offering potential benefits to SDG 13 (Climate Action) by having less effect on the environment. This study further aims to elucidate the underlying mechanisms governing its performance, particularly in relation to pore bridging, filter cake formation, and structural modification of the fluid system.

2. Methodology

For this study, five (5) water-based mud samples were prepared. The samples prepared are shown in Table 1. The analysis parameters are evaluated in relation to the reference conventional mud sample (Control (NaOH)). Fig. 1 outlines the complete experimental procedure, followed in this study from coconut fibre collection and preparation of BCF to mud formulation, physicochemical characterization, and performance evaluation. The concentration range (29–114 g/L) was deliberately selected based on typical dosages reported in previous studies on lignocellulosic and agro-waste-based additives for water-based drilling fluids [28,29]. This range allows systematic evaluation of the transition from beneficial effects at low-to-moderate concentrations to possible over-treatment effects at higher loadings.

2.1. Extraction and preparation of bio-additives

Waste coconut husks were sourced from a local market in Owerri, southeast Nigeria, and the fibres were manually extracted. Following extraction, the fibres were washed with distilled water to remove impurities and then sun-dried for seven days at an ambient temperature of 28–32°C. The sun-dried fibres were then subjected to calcination in a closed oven at 300°C for 3 h. The thermal treatment ensured partial

Table 1
Composition of control and BCF-modified water-based drilling fluids.

Sample	Water (mL)	Bentonite (g)	Barite (g)	CMC (g)	PAC-R (g)	$CaCO_3$ (g)	BCF (g/L)
Control (NaOH)	350	15	28	1.5	0.2	0.25	0
BCF-29	350	15	28	1.5	0.2	0.25	29
BCF-57	350	15	28	1.5	0.2	0.25	57
BCF-86	350	15	28	1.5	0.2	0.25	86
BCF-114	350	15	28	1.5	0.2	0.25	114

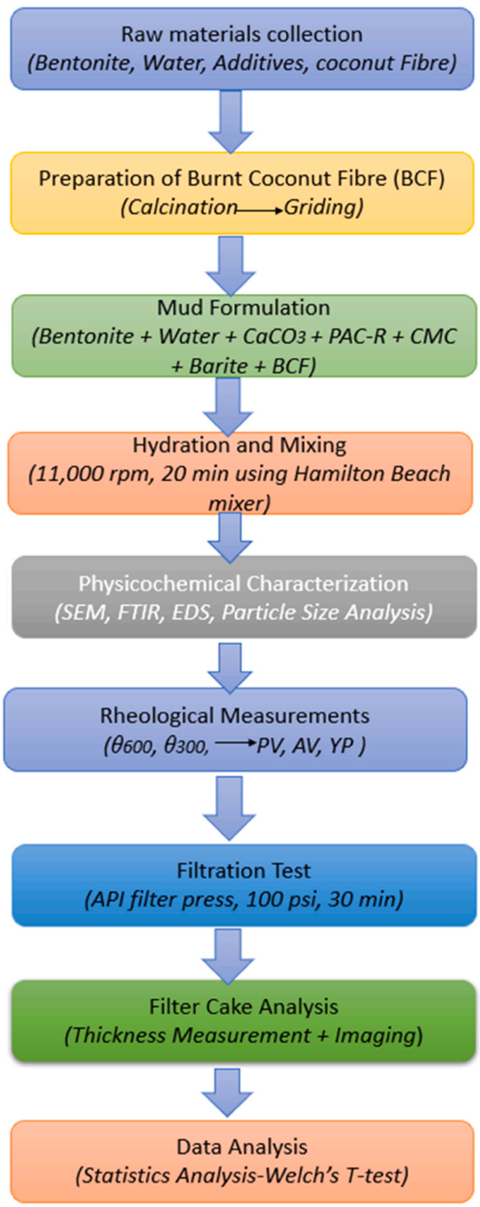

Fig. 1. Flow chart illustrating experimental methodology adopted for the preparation, characterization and evaluation of BCF-modified water-based drilling fluid.

carbonization while retaining essential fibrous characteristics beneficial for drilling fluid performance. In contrast, the sun-drying process ensured that the fibres were free of residual moisture, which could interfere with subsequent thermal processing. After calcination, the fibres were ground into fine ashes using a mechanical grinder to increase their surface area and improve their dispersibility in drilling fluids.

To assess the chemical properties of the BCF in its natural state, the pH of the material was measured prior to sample preparation for SEM analysis. Specifically, 1 g of BCF was dissolved in 10 mL of distilled water, and the pH of the resulting solution was determined using a calibrated pH meter.

For SEM analysis, BCF was prepared by drying the samples and sputter-coating them with a thin layer of gold to enhance electrical conductivity. The samples were then imaged using a UTM IT-300 scanning electron microscope at an accelerating voltage of 5.0 kV, with a working distance ranging from 9.9 to 11.3 mm, under high vacuum conditions. Imaging was conducted at magnifications ranging from ×30 to ×3000 to capture both the overall structure and fine details of the fibre's surface and internal morphology. The SEM images were analyzed to determine pore size distribution, surface roughness, and structural connectivity, which are key factors in assessing the material's performance as a drilling fluid additive.

2.2. Mud preparation

The mud samples were prepared according to the specifications in Table 1. The control mud (Control (NaOH)) contained 0.6 g NaOH as the conventional pH modifier, while BCF was used as an alternative additive in other samples. BCF was added at concentrations of 29, 57, 86, and 114 g/L, corresponding to 10–40 g per 350 mL of base fluid

The preparation process for each mud sample involved precise measurement of components using a weighing balance, followed by thorough mixing with a Hamilton Beach mixer to achieve a homogeneous mixture. For the control mud, the sequence of addition was water, bentonite, carboxymethylcellulose (CMC), polyanionic cellulose (PAC-R), limestone, and barite. For the mud samples containing BCF additives, the sequence was: water, bentonite, BCF (as the additive), CMC, PAC-R, limestone, and barite. Bentonite serves as a crucial component in water-based drilling mud due to its gel-forming properties, which aid in sealing borehole walls and enhancing cuttings transport. CMC was incorporated to minimize water loss and stabilize reactive shales, thereby preventing wellbore collapse through its film-forming capabilities. Limestone functions to control downhole pressure, suspend cuttings, and cool the drill bit during operations. PAC-R was utilized to enhance filtration control and increase the mud's water absorption capacity. Barite and calcium carbonate ($CaCO_3$) were included in all samples as densifying agents to ensure that the resulting mud systems met API standards for density control. Each component was mixed sequentially under controlled stirring conditions, as detailed in the experimental procedure.

The mixing procedure for the mud samples was standardized to ensure consistency across all formulations. Each sample was prepared using 15 g of bentonite dispersed in 350 mL of water. The bentonite was hydrated under continuous stirring at approximately 11,000 rpm for 20 min using a Hamilton Beach mixer to form a uniform base mud. For the control mud, 0.6 g of NaOH was then added and mixed at 11,000 rpm for an additional 10 min. For the BCF-modified samples, the required amount of BCF (29–114 g/L) was added after bentonite hydration and mixed at 11,000 rpm for 10 min. Subsequently, carboxymethyl cellulose (CMC, 1.5 g), polyanionic cellulose regular (PAC-R, 0.2 g), calcium carbonate ($CaCO_3$, 0.25 g), and barite (28 g) were added sequentially, with each component mixed at 11,000 rpm for 10 min to ensure uniform dispersion. The complete mixture was finally stirred at 11,000 rpm for an additional 10 min to achieve homogeneity before rheological and filtration tests were performed.

This standardized high-shear mixing procedure ensured consistent hydration and dispersion across all formulations.

2.3. Particle size characterization

The particle size distribution of the ground BCF was determined by dynamic light scattering (DLS) after dispersing the powder in distilled water at 25 °C. The analysis yielded a Z-average diameter of 1727 nm, with a dominant intensity-weighted peak at approximately 957 nm and a polydispersity index (PDI) of 0.718. This broad distribution, typical of ground carbonaceous biomass materials, indicates a heterogeneous mix of submicron to micron-sized particles. Such a size range is advantageous for drilling fluid applications, as finer particles contribute to pore plugging and filter cake compaction, while larger fibrous fragments enhance bridging and rheological structure. The results are consistent with the porous, fibrous morphology observed in SEM imaging and support the improved filtration control and rheological modifications reported in this study.

2.4. Mud density test

The densities of the mud samples were determined using a 4-scale baroid mud balance according to the following steps: First, the calibration of the balance was verified by referencing the calibration mark on the scale. The mud cup was cleaned, dried, and filled with the prepared mud sample. To eliminate any potential air bubbles trapped within, the lid was carefully placed onto the cup, causing excess mud to overflow. The outer surface of the cup was then wiped clean. Subsequently, the balance was placed on its base, with the knife edges resting upon the fulcrum support. The rider was then adjusted along the balance arm until equilibrium was achieved, visually confirmed by the positioning of a bubble. Once the balance was established, the weight of the mud was read at the point where the filtrate level reached the mark on the graduated cylinder, and this value was duly recorded. The entire procedure was iterated for each distinct mud sample being investigated.

2.5. Viscosity

The rheological properties of the various mud samples were evaluated using the Fann Model 35 Viscometer. Each mud sample was introduced into the viscometer's sample cup, ensuring the rotor sleeve was immersed precisely to the designated fill line by adjusting and securing the platform with the lock nut. The viscometer was then powered on, and the speed control was initially set to the 'STIR' mode to homogenize the sample. Subsequently, the speed was adjusted to 600 rpm, and after allowing the dial reading to stabilize, the measurement was recorded. This procedure was repeated at 300 rpm. The obtained readings were used to calculate plastic viscosity, apparent viscosity, and yield point, in accordance with standard rheological equations [30].

Plastic Viscosity

$$PV = \theta_{600} - \theta_{300} \tag{1}$$

Apparent Viscosity

$$AV = \frac{\theta_{600}}{2} \tag{2}$$

Yield Point

$$YP = \theta_{300} - PV \tag{3}$$

pH Test

The pH levels of diverse mud samples were assessed using a pH meter. Before measurement, the pH meter was calibrated using standard buffer solutions with pH values of 4.0, 7.0, and 10.0 to ensure accuracy across the expected measurement range. Approximately 50 mL of each sample was transferred into a clean, dry beaker. The calibrated electrode was then immersed into the sample, and the solution was gently swirled to ensure homogeneity. The pH reading was allowed to stabilize for 60 s before the value was recorded. Between successive measurements, the electrode was thoroughly rinsed with distilled water to prevent cross-contamination.

2.6. Mud filtration properties

API filtration tests were conducted using a multi-unit filter press at 100 psi for 30 min. The cells were cleaned, assembled with standard components (filter paper, screen, and gasket), and filled with freshly prepared mud samples to approximately 13 mL below the top. Filtrate was collected in graduated cylinders, and the volume was recorded after the test period. The filter cake was recovered and its thickness measured, while the filtrate pH was also determined.

2.7. Permeability estimation

The permeability of the filter cake was estimated using Darcy's law for filtration, shown below

$$k = \frac{Q\mu L}{A\Delta Pt} \tag{4}$$

where k is the permeability, Q is the filtrate volume is the filtrate viscosity (assumed as 1 cP), L is the filter cake thickness, and A is the filtration area (45.8 cm^2). ΔP is the applied pressure, and t is the filtrate time.

All experiments were performed in triplicate ($n = 3$) to ensure reproducibility. Each replicate followed the identical formulation and testing protocol described above. Measured parameters (density, plastic viscosity, apparent viscosity, yield point, gel strength, fluid loss, mud-cake thickness, pH) are reported as mean ± standard deviation (SD). All rheological and filtration measurements were conducted at ambient laboratory temperature of 25 °C

3. Results and discussion

The SEM images of BCF (Fig. 2) reveal a highly porous, three-dimensional structure with interconnected pores, observed at magnifications of × 430, × 1000, × 1500, × 2500, and × 3000. This porous and irregular morphology plays a crucial role in filtration control by facilitating mechanical interlocking with bentonite particles and promoting effective pore bridging at the filter medium interface. During filtration, BCF particles initially block larger pore throats (spurt loss control), while finer fragments and ash residues fill interstitial voids, forming a compact, low-permeability filter cake.

This multiscale packing mechanism restricts fluid flow through the cake matrix, thereby reducing filtrate invasion into the formation [31]. At a higher magnification of ×3000, as shown in Fig. 2(a), the surface of the BCF fibre exhibits a rough, irregular texture with microscale protrusions, which could enhance particle bridging and sealing in fractured or porous formations. The rough surface morphology likely results from the calcination process, which removes organic components and leaves behind a textured, inorganic-rich structure. This microstructure supports the idea that BCF can serve as an effective additive for bridging, reducing filtration loss, and possibly inhibiting shale in water-based mud systems.

At lower magnifications of ×1000 and ×430 shown in Fig. 2(d) and Fig. 2(e), the overall fibrous structure of BCF is evident, showing a layered, elongated morphology. Despite the calcination and grinding processes, the material retains a fibrous network, which can contribute to the mechanical strength of the drilling fluid, potentially improving its ability to suspend cuttings and maintain wellbore stability. The interconnected nature of the pores also suggests that BCF could enhance the

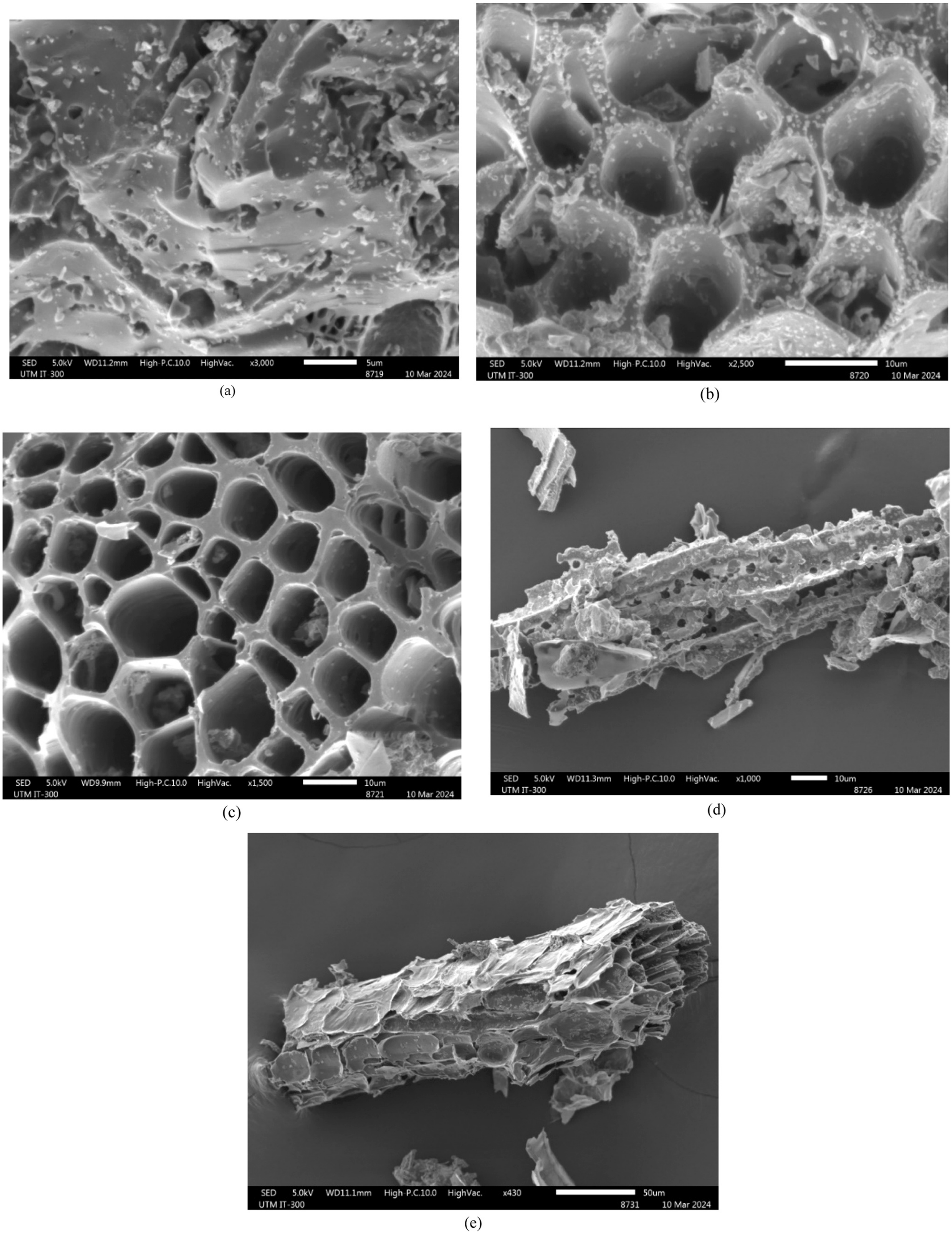

Fig. 2. Scanning electron micrographs of BCF at magnifications of (a) ×3000, (b) ×2500, (c) ×1500, (d) ×1000, and (e) ×430, showing porous and fibrous morphology. The micrographs illustrate surface roughness and interconnected pore structure, which contribute to pore bridging and filter cake formation in drilling fluid systems.

rheological properties of water-based drilling fluids by increasing viscosity and yield point, which are essential for efficient cuttings transport.

The calcination process at 300 °C likely enhanced the thermal stability of the coconut fibre, making it more suitable for high-temperature drilling environments compared to its unprocessed form. However, the SEM images also reveal some limitations. The irregular pore size distribution and the presence of fine debris on the fibre surface, visible at ×3000 magnification, may lead to inconsistent performance in drilling fluids. Additionally, while the calcination process improves thermal stability, the biodegradability of the lignocellulosic material may still pose challenges in extremely high-temperature, high-pressure (HTHP) conditions, where further degradation could occur. The pH analysis of BCF in its natural state provides insight into its chemical behavior, which is critical for ensuring compatibility with other drilling fluid components, such as polymers and weighting agents.

3.1. *Fourier transform infrared spectroscopy (FTIR) analysis*

The FTIR spectrum of BCF, shown in Fig. 3, revealed distinct absorption peaks that confirm the presence of functional groups relevant to drilling mud enhancement. A broad band around 3340 cm^{-1} corresponds to O–H stretching vibrations from hydroxyl groups, indicative of cellulose and residual lignin content [32]. Peaks observed near 2915 cm^{-1} represent aliphatic C–H stretching, while the strong absorption at approximately 1605 cm^{-1} signifies C═C or aromatic skeletal vibrations, confirming partial carbonization and the presence of aromatic structures [33,34]. Additional bands at 1030 cm^{-1} and 1240 cm^{-1} are attributable to C–O–C and C–O stretching, respectively, associated with hemicellulose and lignin remnants [35,36]. These functionalities suggest the material retains surface reactivity and structural features necessary for interaction with clay particles and water molecules in a drilling fluid matrix. To evaluate the effect of thermal treatment on BCF, the FTIR spectrum of the BCF used in this study was compared with published spectra of raw coconut fibre. The comparison is presented in Table 2, as shown, BCF retains major hydroxyl (O-H) and ether (C-O-C) groups observed in raw fibre, with notable reductions in the C═O and aromatic C═C bands, which are typically associated with hemicellulose and lignin. The attenuation or disappearance of these peaks in BCF indicates partial decomposition of

Table 2
Comparative FTIR peak assignment of raw and burnt coconut fibre, highlighting major functional groups changes due to thermal treatment.

Wavenumber (cm^{-1})	Raw Coconut Fibre Freitas et al. [41]	Burnt Coconut Fibre (This study)	Interpretation
~3340	Broad O–H stretching (cellulose, lignin)	Broad O–H stretching	Retained hydroxyl groups.
~2915	Aliphatic C–H stretching	Aliphatic C–H stretching	Common in lignin/ hemicellulose; presence in both indicates partial preservation
~1730	C═O stretching (hemicellulose)	Absent or reduced	Suggests degradation of hemicellulose during burning
~1600–1610	Aromatic C═C skeletal vibration	Aromatic skeletal vibration (~1605)	Enhanced aromatic character due to carbonization
~1510–1520	Lignin-related aromatic ring vibrations	Weak or absent	Indicates breakdown of lignin structure with heat
~1240–1260	C–O stretching (lignin)	Present (~1240)	Still present in burnt fibre, suggesting partial degradation
~1030–1040	C–O–C stretching (cellulose/ hemicellulose)	Present (~1030)	Indicates retention of polysaccharide structures

hemicellulose and skeletal vibration band (1600 nm) also suggests increased aromatic character due to carbonization. The chemical functionality is further supported by the Energy Dispersive X-ray Spectroscopy (EDS) analysis shown in Table 3, which indicates a dominant carbon content (82.7 wt%), consistent with effective carbonization of lignocellulosic biomass [37]. Oxygen (8.7 wt%) supports the presence of functional groups such as hydroxyl and carbonyl, as confirmed by FTIR bands around 3300 cm^{-1} and 1000 cm^{-1}. These functional groups contribute to hydration, swelling, and particle interaction within the mud, which are critical for suspension and filtration control.

Notably, potassium (4.6 wt%) and chlorine (2.4 wt%), present in higher quantities, suggest the additive's potential contribution to ionic strength and cation exchange in clay-based drilling systems [38].

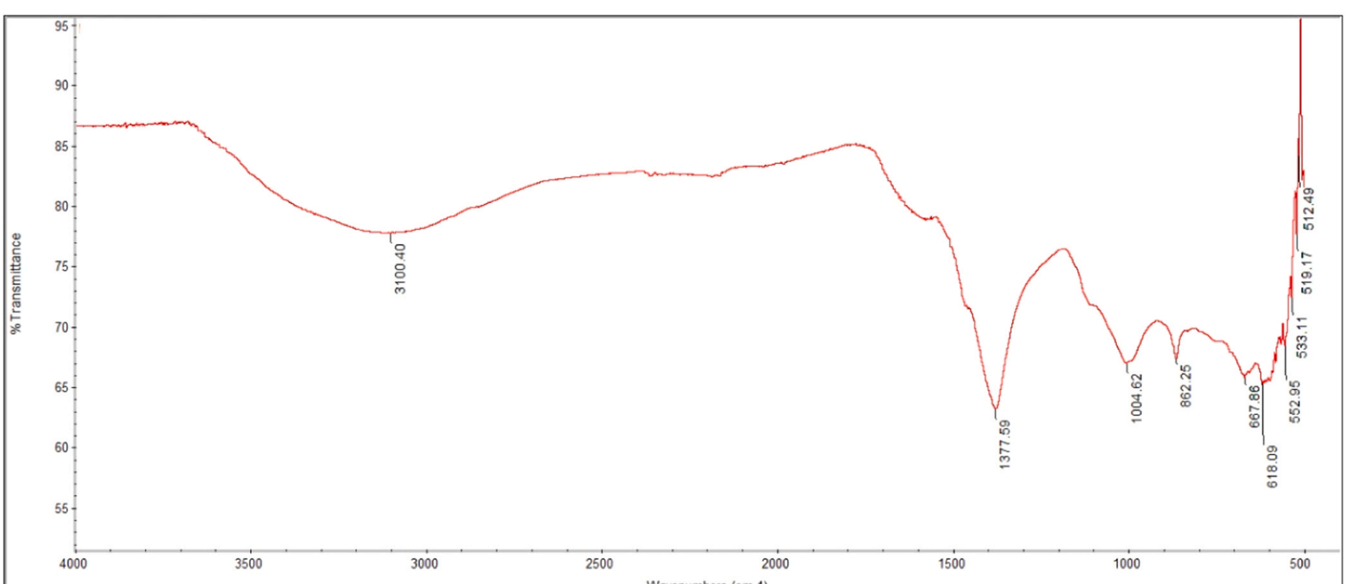

Fig. 3. Fourier Transform Infrared (FTIR) spectrum of BCF showing characteristic functional groups indicative of lignocellulosic components and carbonaceous structures relevant to its evaluation as a potential drilling mud additive.

Table 3
Elemental composition of BCF from EDS analysis.

Element	Weight Percentage (wt%)
Carbon (C)	82.7
Oxygen (O)	8.7
Potassium (K)	4.6
Chlorine (Cl)	2.4
Aluminium (Al)	0.8
Sodium (Na)	0.3
Silicon (Si)	0.2
Magnesium (Mg)	0.1
Iron (Fe)	0.1
Sulfur (S)	0.1

Potassium ions have also been widely recognized for their ability to reduce clay swelling in reactive shales through cation exchange and osmotic effects, although their efficacy is often limited by concentration thresholds and methodological variability [39,40]. Trace levels of aluminium, sodium, silicon, magnesium, iron, and sulphur further enhance the additive's profile, indicating a mixture of organic and inorganic character that can influence the fluid's pH, gel strength, and interaction with other mud components.

3.2. Thermogravimetric analysis (TGA) and differential thermal analysis (DTA)

The suitability of BCF as a drilling fluid additive was further evaluated based on its thermal degradation behavior obtained from thermogravimetric analysis (TGA). The TG and DTG profiles shown in Fig. 4 reveal that BCF exhibits minimal mass loss below approximately 120 °C, which is primarily ascribed to the removal of physically adsorbed moisture. This indicates that the material maintains structural integrity under low to moderate thermal conditions typically encountered in shallow to intermediate drilling operations. The onset of significant thermal degradation occurs at temperatures above 200 °C, corresponding to the decomposition of lignocellulosic constituents, including hemicellulose, cellulose, and lignin. Since the majority of water-based drilling fluids operate at temperatures well below this degradation threshold, BCF demonstrates adequate thermal stability for use as a drilling fluid additive without premature thermal breakdown. Furthermore, the gradual mass loss beyond 400 °C, accompanied by a substantial residual char yield at elevated temperatures, reflects the fibre's lignin-rich composition and inherent resistance to thermal collapse. The formation of thermally stable char suggests that BCF can withstand transient temperature spikes without catastrophic degradation, an important consideration for downhole environments subject to thermal fluctuations.

3.3. Size distribution by intensity

The particle size distribution obtained from dynamic light scattering (DLS) analysis (Fig. 5) exhibits a single dominant intensity peak, suggesting an apparently monomodal distribution of BCF particles dispersed in water. The results yielded a Z-average diameter of 1727 nm with a dominant intensity-weighted peak at approximately 957 nm. The measured polydispersity index (PDI) of 0.718 indicates a broad particle size distribution, which is a hallmark attribute of heterogeneous, carbonaceous biomass-derived materials. The intensity-based size distribution reveals a single dominant peak, suggesting that the system is primarily governed by submicron to micron-sized particles rather than a mixture of widely separated particle populations. The relatively high Z average compared to the peak position reflects the sensitivity of cumulant analysis to larger particles and weak agglomerates, which is typical of non-spherical and irregular materials such as thermally degraded natural fibres [42,43]. The high intercept value (0.925) confirms good signal quality and measurement reliability, indicating sufficient particle concentration and stable scattering conditions during analysis. The presence of particles in the 1 μm range shows that thermal treatment of BCF transforms the original fibrous structures into fragmented carbonaceous particles, rather than complete volatilization or collapse. This observation is consistent with the TGA results, which showed substantial char residue at elevated temperatures, confirming the formation of thermally stable solid products. The relatively high PDI reflects the non-uniform fragmentation behavior of lignocellulosic

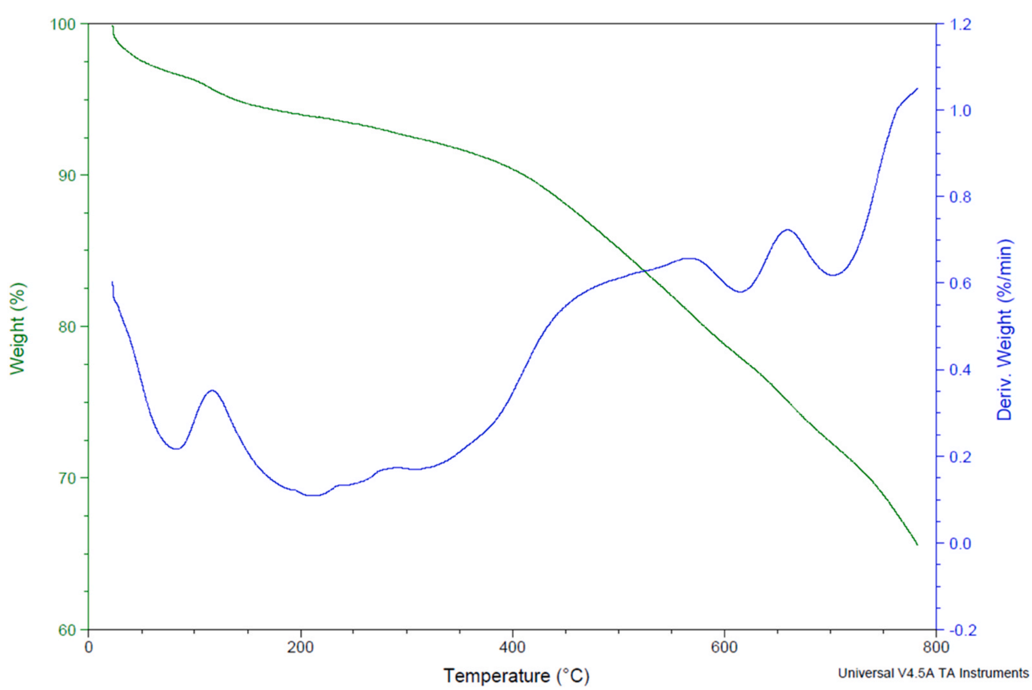

Fig. 4. Thermogravimetric (TG) and derivative thermogravimetric (DTG) curves of BCF showing multi-stage thermal degradation behavior. The initial mass loss below 120 °C corresponds to moisture evaporation, while the major decomposition region between 200 and 400 °C is associated with the degradation of lignocellulosic components.

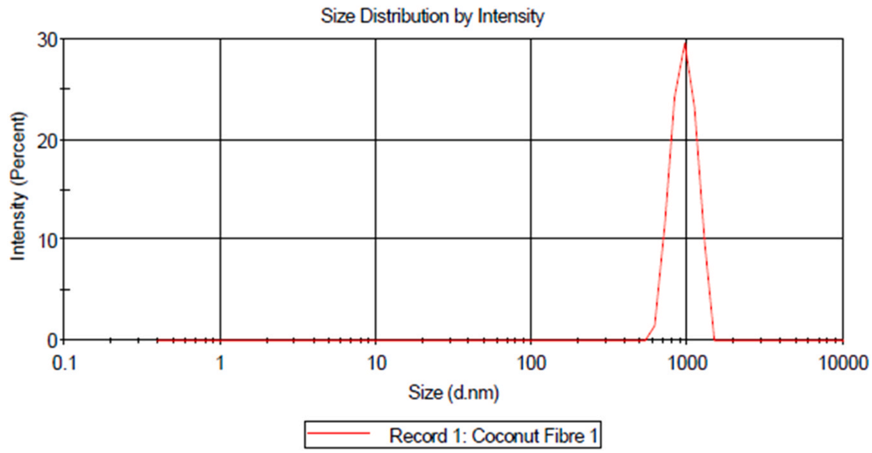

Fig. 5. Particle size distribution of BCF obtained by dynamic light scattering (DLS), showing intensity-weighted size distribution and dominant particle size in the submicron range.

materials during thermal degradation, which results in a distribution of particle sizes rather than monodisperse nanoparticles. Such heterogeneity is expected and acceptable for drilling-fluid additives, where functionality is governed more by bridging and packing effects rather than by monodispersity. The measured particle size confirms that grinding after calcination produced a suitable range for effective bridging and filtration control, as finer particles aid in reducing fluid loss while the fibrous network supports yield point development.

3.4. Mud density

Table 4 summarizes the measured densities of the mud systems, while Fig. 6 visualizes the same data to illustrate the progressive increase in mud weight with BCF concentration. As shown, the control mud has a density of 8.59 ± 0.06 ppg. Density progressively increased with BCF concentration, reaching 9.13 ± 0.05 ppg at 114 g/L. The increase was statistically significant compared to the control (Welch's *t*-test, two-tailed, unequal variance). Additionally, all mud densities remain within the API-recommended range (8.45–9.5 ppg) for normally pressured formations [44]. This suggests that BCF can achieve moderate density improvement without risking excessive equivalent circulating density (ECD) that can result in lost circulation.

The same observation also indicates that BCF not only contributes to fluid structuring but also to the total mud weight. The progressive densification can be considered a result of the presence of carbonaceous and mineral-rich residue within the fibre matrix, as evidenced by FTIR analysis, with the presence of hydroxyl, carbonyl, and aromatic groups. These functional groups promote hydration, dispersion, and inter-particle interactions within the mud system.

SEM micrographs of the additive revealed a highly porous and fibrous microstructure with irregular topography and microcracks. This morphology enhances the surface area, facilitating increased interaction with water molecules and clay particles, which likely contributed to the observed increase in mud viscosity and density. The structural roughness also suggests a potential bridging mechanism, where the fibres help in forming a more compact mud matrix capable of minimizing filtrate invasion and stabilizing the borehole wall.

Table 4
Mud density of water-based drilling fluid samples (mean ± SD, n = 3).

Mud Sample	Concentration of additive (g/L)	Mud Density mean ± SD (ppg)	p value (vs control)
Control (NaOH) (conventional/ control)	-	8.59 ± 0.06	Conventional NaOH
BCF-29	29	8.94 ± 0.04	0.003*
BCF-57	57	9.03 ± 0.09	0.003*
BCF-86	86	9.09 ± 0.09	0.002*
BCF-114	114	9.13 ± 0.05	0.0004*

* $p < 0.05$ (Welch's *t*-test, two-tailed, unequal variance).

3.5. Rheological behavior of BCF-modified drilling fluids

The rheograms presented in Fig. 7 illustrate the relationship between shear stress and shear rate for the control and BCF-modified drilling fluid systems. In all cases, shear stress increases with increasing shear rate, confirming the non-Newtonian behavior of the fluids, consistent with typical water-based drilling muds.

The control sample exhibits the highest shear stress at 1022 s^{-1}, indicating greater resistance to flow at high shear conditions. In contrast, BCF-modified samples show comparatively lower shear stress values at higher shear rates, particularly at elevated BCF concentrations (BCF-86 and BCF-114), suggesting a reduction in flow resistance and improved shear-thinning behavior.

At a lower shear rate (511 s^{-1}), Samples BCF-29 and BCF-57 exhibit higher shear stress compared to the control, indicating enhanced structural integrity and yield behavior. This suggests that the addition of BCF at low to moderate concentrations improves interparticle interactions, thereby enhancing the fluid's ability to suspend drill cuttings under low shear conditions.

The near-linear relationship between shear stress and shear rate across all samples supports the applicability of the Bingham plastic model. The reduction in slope observed in BCF-modified systems reflects decreased plastic viscosity, while the elevated intercept at lower concentrations indicates improved yield point. However, at higher BCF concentrations, the reduction in both slope and intercept suggests excessive thinning of the fluid structure.

Overall, the rheological response demonstrates that BCF acts as an effective rheology modifier, with optimal performance observed at low to moderate concentrations (29–57 g/L), where a balance between flowability and structural strength is achieved.

Fig. 8 and Table 5 summarize the key Bingham plastic parameters (plastic viscosity, apparent viscosity, and yield point) of the control and BCF-modified drilling fluid samples. As shown in Fig. 8, control (NaOH) exhibited the highest plastic viscosity (PV) of 31.5 ± 0.10 cP. In contrast, all BCF-containing formulations displayed a substantial and progressive reduction in PV, ranging from 14.07 ± 1.01 cP for BCF-29 to 8.33 ± 0.29 cP for BCF-114. This consistent decrease in PV with increasing BCF concentration indicates a thinning effect, which reduces viscous drag and lowers the energy required for mud circulation and pumping. Lower PV values are advantageous for minimizing circulating

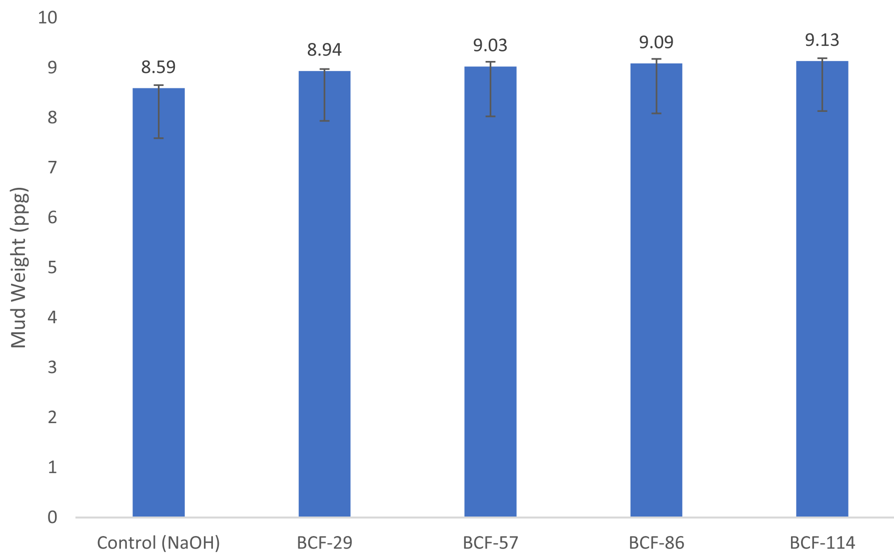

Fig. 6. Mud density (ppg) of various mud samples with varying BCF concentrations (mean ± SD, n = 3). Error bars represent ±1 standard deviation.

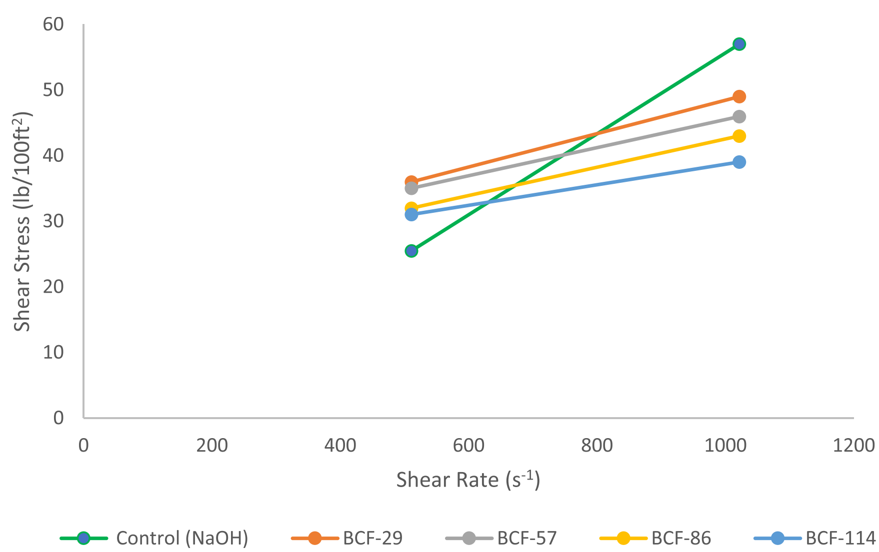

Fig. 7. Rheogram showing the relationship between shear stress (τ) and shear rate (γ) for the control mud and BCF-modified muds at different concentrations. The plots demonstrate the shear-thinning (pseudoplastic) behavior of all mud samples.

pressures and pump horsepower demands during drilling operations. All BCF-treated samples exhibited significantly lower PV compared to the control ($p < 0.01$).

Apparent viscosity (AV) followed a similar trend, decreasing from 23.93 ± 0.51 cP in the control to values between 19.55 ± 1.63 cP (BCF-29) and 15.50 ± 0.20 cP (BCF-114). BCF-57 and BCF-86 showed relatively stable AV behavior within this range. The reduction in AV was statistically significant ($p < 0.05$ for Sample I; $p < 0.01$ for BCF 29-BCF 114). These results highlight the dual role of BCF as an additive: it decreases frictional resistance at high shear rates (contributing to lower PV and AV) while enhancing low-shear flow resistance, which supports improved cuttings suspension.

Yield point (YP) values further underscore the beneficial rheological impact of BCF. The control mud displayed a negligible YP, indicative of limited gel structure and cuttings-carrying capacity. In contrast, BCF incorporation markedly increased YP to 22.23–23.73 lb/100 ft^2, with the highest value observed in BCF-57 (23.73 ± 0.25 lb/100 ft^2). All BCF-modified samples exhibited significantly elevated YP compared to the control ($p < 0.01$). This enhancement improves the mud's ability to suspend and transport drill cuttings through the annulus under static or low-shear conditions, without exceeding typical industry limits that could lead to issues such as excessive pressure losses, differential sticking, or gel-bed formation.

The YP/PV ratio was assessed to better understand the rheological behavior of the drilling fluids. Conversely, BCF-modified systems exhibited a significant increase in YP/PV, due to the combined effect of reduced plastic viscosity and relatively high yield point. This suggests an enhanced cutting transport across all BCF concentrations. Several authors have studied the ideal YP/PV range, with studies by Okrajni [45] suggesting 0–2, while Gautam et al. [46] suggest 1–2. However, excessively high YP/PV value observed at higher BCF loading (40 g) may indicate over-structuring of the fluid, which could adversely affect flow behavior and circulation efficiency. Therefore, optimal performance is achieved at low to moderate BCF concentrations (29–86 g/L), where a balance of flowability and suspension capacity is maintained. The higher YP/PV ratios suggest that BCF improves hole cleaning efficiency while maintaining lower flow resistance, making it advantageous for optimized drilling performance.

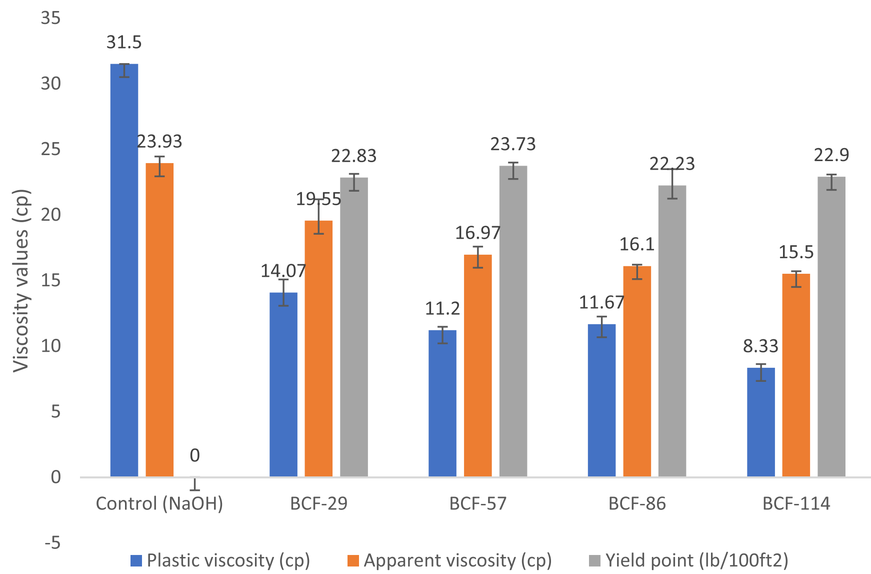

Fig. 8. Plastic viscosity (PV), apparent viscosity (AV), and yield point (YP) of control and BCF-modified drilling fluids as a function of BCF concentration. PV, AV, and YP are reported in cP. Values represent mean ± standard deviation (n = 3).

Table 5
Summary of the plastic viscosity (PV), apparent viscosity (AV), and yield point (YP) results of the control mud and drilling fluids formulated with varying concentrations of BCF (mean ± SD, n = 3).

Sample	Plastic Viscosity (cP)	Apparent Viscosity (cP)	Yield Point (cP)	Notes / Significance vs Control
Control (NaOH)	31.5 ± 0.10	23.93 ± 0.51	0	-
BCF-29	14.07 ± 1.01	19.55 ± 1.19	22.83 ± 0.29	PV: $p < 0.01$ YP: $p < 0.01$; AV: $p < 0.05$
BCF-57	11.2 ± 0.26	16.97 ± 0.61	23.73 ± 0.25	PV: $p < 0.01$ YP: $p < 0.01$ AV: $p < 0.01$
Sample BCF-86	11.67 ± 0.58	16.1 ± 0.1	22.23 ± 1.25	PV: $p < 0.01$ YP: $p < 0.01$ AV: $p < 0.01$
BCF-114	8.33 ± 0.29	15.5 ± 0.2	22.9 ± 0.17	PV: $p < 0.01$ YP: $p < 0.01$ AV: $p < 0.01$

$p < 0.01$, *$p < 0.05$ vs control (Welch's *t*-test, two-tailed, unequal variance, n = 3).

The rheological properties of the drilling fluid systems were evaluated in relation to standard field guidelines. The plastic viscosity values for the BCF-modified samples fall within or below the typical operational range (10–35 cP), indicating reduced flow resistance and improved pumpability. Yield point values remained within acceptable limits, suggesting adequate interparticle interaction for cuttings suspension.

In summary, the addition of BCF at concentrations of 29–57 g/L significantly reduced plastic and apparent viscosities while substantially increasing yield point ($p < 0.01$ for PV and YP across all samples; while $p < 0.05$ to $p < 0.01$ for AV depending on dose. These rheological improvements align with prior observations that certain bio-additives, including fibrous materials, can function as thinning agents in water-based mud systems while enhancing suspension properties [47]. The observed trends suggest that BCF may provide an effective means of optimizing mud rheology to improve drilling performance.

3.6. Gel strength

Gel strengths (10-second initial and 10-minute progressive) of water-based mud samples are shown in Fig. 9 and summarized in Table 6. The control mud exhibited high gel strength values at 10 s and 10 min, measuring 32.67 ± 0.57 lb/100 ft^2 and 37.67 ± 1.41 lb/100 ft^2, respectively, indicating the formation of a strong gel structure under static conditions. A noticeable decrease was observed in BCF-29 with values dropping to 17.33 ± 1.53 lb/100 ft^2 and 26.07 ± 0.71 lb/100 ft^2 for 10 s and 10 min, respectively. This suggests that low concentrations of BCF initially weaken the gel network, probably by improving particle dispersion and disrupting excessive clay-to-clay interactions. As BCF concentration increases in samples BCF-57 to BCF-114, gel strength values also increase. The 10-second gel strength rises from 22.27 ± 0.38 to 27.53 ± 0.5 lb/100 ft^2, and the 10-minute gel strength increases from 32.67 ± 1.41 to 36.80 ± 0.82 lb/100 ft^2. This indicates that the additive helps the mud develop a stable gel structure under shear stress. The trend shows a gradual formation of a stable yet controllable gel as BCF concentration rises, due to enhanced interparticle interactions and network formation involving the fibrous char particles. Statistical comparisons to the control were conducted using a two-tailed Welch's *t*-test assuming unequal variances. The 10-s gel strength decreased significantly in all BCF-modified samples ($p < 0.05$). Conversely, the 10-min gel strength showed a significant reduction only at low concentrations (BCF-29, $p < 0.05$); at higher concentrations, the differences were not statistically significant ($p > 0.05$), indicating a recovery toward control behavior.

This progressive enhancement in gel strength with increasing BCF concentration is strongly correlated with the fibre's microstructural and chemical characteristics. SEM imaging revealed a porous, fibrous microstructure with rough surface features that increase available surface area and promote mechanical interlocking between particles in the mud. Simultaneously, FTIR analysis confirmed the presence of hydroxyl and carbonyl groups, which enable hydrogen bonding and improved water retention, fostering better interaction with clay particles. Additionally, elemental analysis showed appreciable levels of potassium and sodium, which support dispersion and flocculation of clay platelets, thereby reinforcing the gel matrix. Together, these attributes enhance the mud's ability to form a cohesive, yet flexible gel network that effectively suspends drill cuttings during static conditions.

The relatively subdued gel properties inherent to muds fortified with BCF offer advantageous attributes for operational viability within

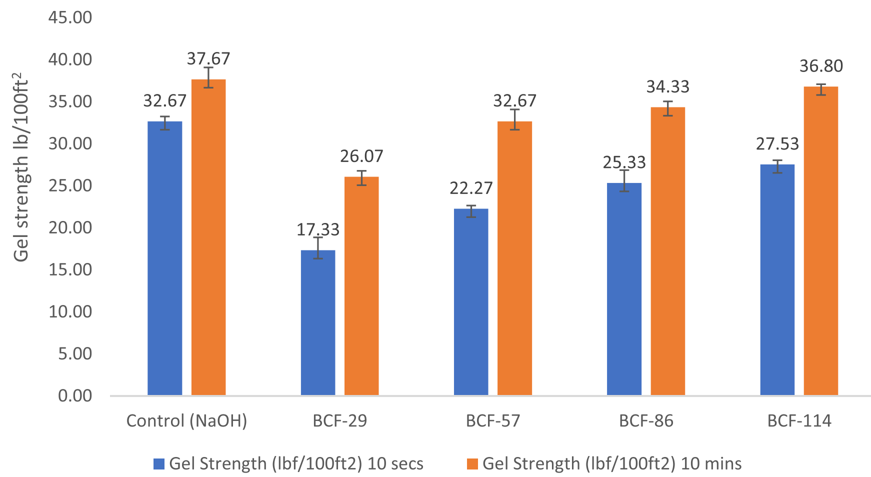

Fig. 9. Ten-second and ten-minute gel strength of control and BCF-modified water-based drilling fluids at varying BCF concentrations. Gel strength values are reported in lb/100 ft^2. Error bars represent the standard deviation of triplicate measurements (n = 3).

Table 6
Gel strength (10 s and 10 min) of water-based drilling mud samples (mean ± SD, n = 3).

Sample	Gel Strength 10 s (lb/100 ft^2)	Gel Strength 10 min (lb/100 ft^2)	Significance vs Control (10 s)	Significance vs Control (10 min)
Control (NaOH)	32.67 ± 0.57	37.67 ± 1.41	—	—
BCF-29	17.33 ± 1.53	26.07 ± 0.71	$p < 0.05$	$p < 0.05$
BCF-57	22.27 ± 0.37	32.67 ± 1.41	$p < 0.05$	$p < 0.05$
BCF-86	25.33 ± 1.53	34.33 ± 0.70	$p < 0.05$	$p < 0.05$
BCF-114	27.53 ± 0.50	36.80 ± 0.28	$p < 0.05$	$p > 0.05$ (ns)

Notes: ns = not significant ($p > 0.05$).

drilling operations. These gel structures display an aptitude for facile disruption under lower pump pressures, facilitating unimpeded circulation [48]. Contrastingly, the elevated gel strength values evident in muds containing sodium hydroxide engender heightened circulation breakdown pressures, coupled with augmented pumping costs due to the necessitated high pump power required to counterbalance the pronounced gelling tendencies [49].

To optimize hole cleaning and manage surge/swab pressures, field best practices recommend maintaining 10-second gel strengths within 2–10 lb/100 ft^2 and 10-minute gel strengths within 6–30 lb/100 ft^2. The gel strengths recorded in this study were within these recommended limits, indicating sufficient cutting suspension.

3.7. pH of the mud samples

pH values of the water-based mud samples are presented in Fig. 10 and summarized in Table 7. The Control (NaOH)) exhibited a strongly alkaline pH of 10.03 ± 0.95, typical of NaOH-treated water-based drilling fluids. Addition of BCF significantly lowered the pH to 8.10 ± 0.10 for BCF-29, with values remaining in a narrow range of 8.20 ± 0.30–8.47 ± 0.49 for BCF-59 to BCF-114.

Welch's *t*-test showed that the pH reductions relative to the control were not statistically significant ($p > 0.05$ in all cases). Differences among the BCF-containing samples themselves were also not statistically significant ($p > 0.05$), indicating that BCF concentration has only a

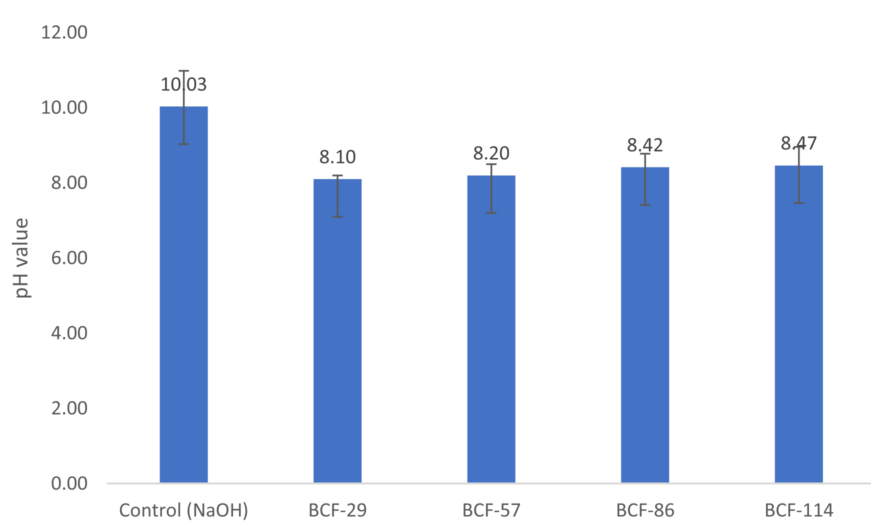

Fig. 10. pH values of control and BCF-modified water-based drilling fluids at varying BCF concentrations. Values are reported as mean ± standard deviation of triplicate measurements.

Table 7
Influence of BCF concentration on drilling fluid pH: mean values and statistical significance.

Sample	pH Value	Significance vs Control
Control (NaOH)	10.03 ± 0.95	—
BCF-29	8.10 ± 0.10	p > 0.05 (ns)
BCF-57	8.20 ± 0.30	p > 0.05 (ns)
BCF-86	8.42 ± 0.36	p > 0.05 (ns)
BCF-114	8.47 ± 0.49	p > 0.05 (ns)

modest influence on final pH within the 29–114 g/L range tested.

This moderate rise in pH is attributed to the presence of alkali metals such as potassium (4.6 wt%) and sodium (0.3 wt%) identified through elemental analysis of the BCF shown in Table 3. These elements, present in the ash residue of the thermally treated fibre, dissociate in solution to contribute hydroxide ions, thus mildly elevating the mud's alkalinity [50,51].

Additionally, the FTIR spectrum confirmed oxygen-rich functional groups such as hydroxyl and carbonyl, which enhance the material's buffering capacity and help maintain chemical stability within the mud system. Unlike sodium hydroxide, which causes an abrupt and strong pH shift, BCF exerts a more controlled and gradual modulation of pH, supporting stable fluid behavior and minimizing the risk of over-alkalinization. According to API guidelines, the acceptable pH range for water-based muds is typically 8.5–10.5. All samples in this study fell within or near this range, confirming compatibility.

3.8. *Filtration loss test*

The proposed mechanism for control of filtration in BCF-enhanced fluids is illustrated in Fig. 11. The fibrous structure of BCF promotes initial bridging of pore throats, followed by a progressive filling of interstitial voids by finer particles. This results in the formation of a compact, low-permeable filter cake. Additionally, the fibrous network encourages interparticle interactions within the fluid, contributing to improved rheological behavior and cuttings suspension. Fig. 12 represents the filtrate volume from the formulated muds collected after 5, 10, and 15 min. The control mud exhibits filtration losses of 5.53 ± 0.46, 6.63 ± 0.55, and 8.87 ± 0.77 mL at 5, 10, and 15 min, respectively. These values indicate moderate filtrate invasion and the formation of a relatively permeable filter cake [52].

A general reduction in filtration loss with increasing BCF concentration was observed, particularly at longer filtration times. At 15 min, the control mud exhibited a fluid loss of 8.87 ± 0.77 mL, the BCF modified muds showed comparable or reduced filtrate volumes, with BCF-29 recording a slightly higher value of 8.88 ± 0.33 mL, while BCF-57, BCF-86, and BCF-114 recorded progressively lower fluid losses of 8.17 ± 0.15 mL, 7.73 ± 0.20 mL, and 7.60 ± 0.52 mL, respectively. Notably, BCF-114 exhibits the lowest filtration loss at extended filtration time, indicating improved fluid-loss control at higher BCF concentrations. This suggests that higher concentrations of the BCF additive contribute to improved fluid retention and reduced fluid loss into the formation. At the early stage of filtration (5 min), the BCF-modified muds exhibited lower filtrate volumes compared to the control sample. The reduction in early-stage filtration suggests improved control of spurt loss, which is critical in minimizing rapid fluid invasion during initial filter cake formation.

The control mud recorded a filtrate volume of 5.53 ± 0.46 mL, which increased to 5.90 ± 0.08 mL and 5.91 ± 0.07 mL for BCF-29 and BCF-57, respectively. A reduction was observed for BCF-86 and BCF-114, with filtrate volumes of 4.90 ± 0.09 mL and 4.99 ± 0.1 mL, respectively.

Statistical analysis of filtration loss was conducted using Welch's *t*-test to compare each BCF-containing sample with the control at 5, 10, and 15 min (Table 8). At 5 min, no statistically significant reductions were observed for any BCF sample (all p > 0.13; range: 0.14–0.30). At 10 min, significant reductions were detected for BCF-29 (p = 0.020) and II (p = 0.041), whereas BCF-86 and BCF-114 did not differ significantly

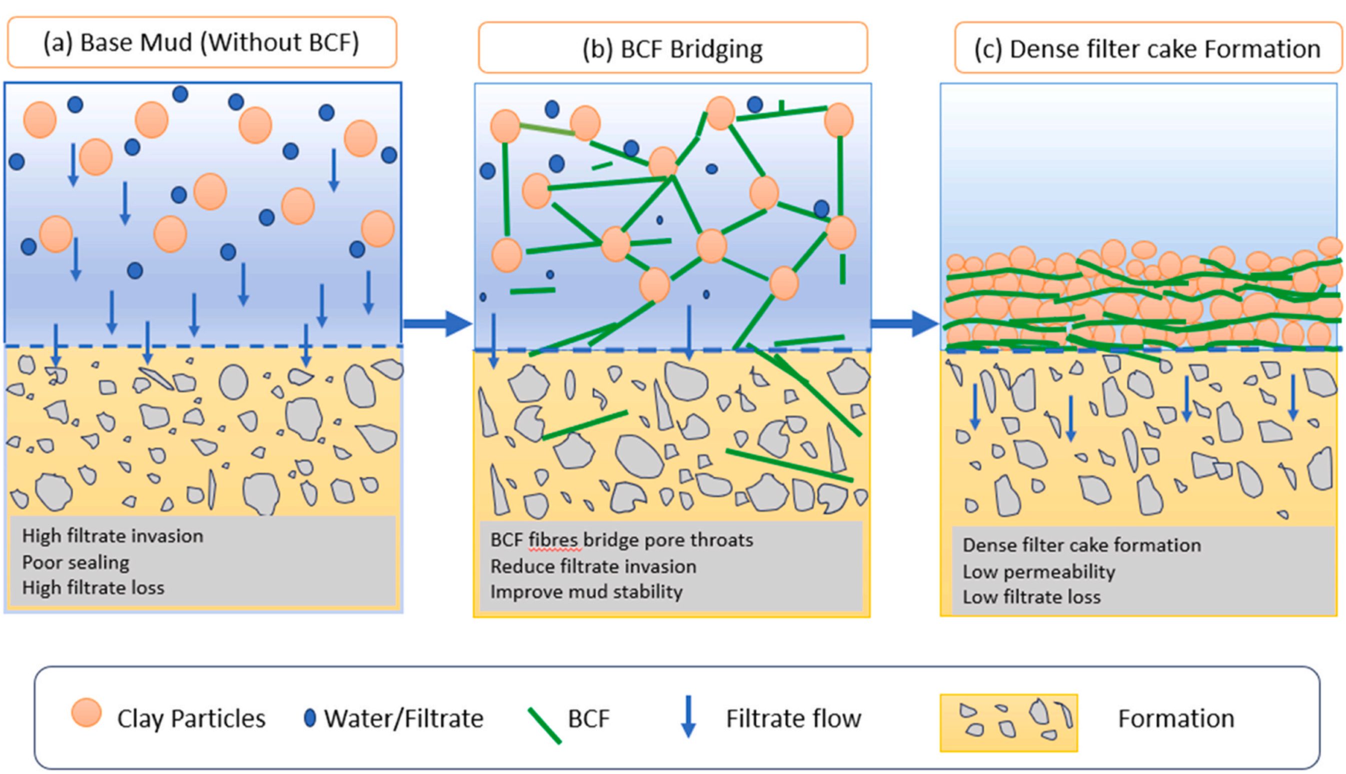

Fig. 11. Schematic illustration of the mechanism of BCF in water-based drilling fluids, showing pore bridging, particle packing, and formation of a low-permeability dense filter cake that reduces filtrate invasion.

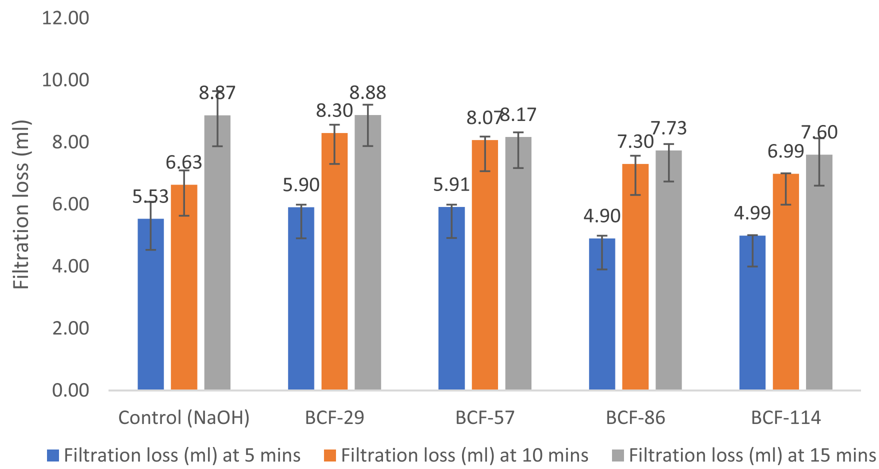

Fig. 12. API filtration loss of control and BCF-modified water-based drilling fluids measured at 5, 10, and 15 min under a constant pressure of 100 psi. Filtrate volumes are presented as mean ± standard deviation (n = 3).

Table 8
Time-dependent API filtration loss and statistical significance of BCF-modified drilling fluids.

Sample	5 min (mL)	Significance (5 min)	10 min (mL)	Significance (10 min)	15 min (mL)	Significance (15 min)
Control (NaOH)	5.53 ± 0.46	—	6.63 ± 0.55	—	8.87 ± 0.77	
BCF-29	5.90 ± 0.08	p > 0.05 (ns)	8.30 ± 0.26	p < 0.05*	8.88 ± 0.33	p > 0.05 (ns)
BCF-57	5.91 ± 0.07	p > 0.05 (ns)	8.07 ± 0.11	p < 0.05*	8.17 ± 0.15	p > 0.05 (ns)
BCF-86	4.90 ± 0.08	p > 0.05 (ns)	7.30 ± 0.26	p > 0.05 (ns)	7.73 ± 0.20	p > 0.05 (ns)
BCF-114	4.99 ± 0.01	p > 0.05 (ns)	6.99 ± 0.01	p > 0.05 (ns)	7.60 ± 0.52	p > 0.05 (ns)

Notes:

- ns = not significant ($p > 0.05$); *$p < 0.05$.
- All filtration losses remain well below typical API limits (e.g., <15 mL at 30 min), indicating good overall fluid-loss control.

from the control ($p > 0.11$). By 15 min, filtration losses for all BCF samples remained statistically comparable to the control (all $p > 0.08$; range of 0.086–0.98), with the lowest p value observed for BCF-114.

Overall, these results indicate that BCF reduces filtration volumes in a dose-dependent manner; however, statistically significant effects were observed only at the 10-minute interval for the lower BCF concentrations (29–57 g/L).

In addition to filtrate volume, filter cake thickness was evaluated to provide further insight into filtration performance. The results indicate that BCF-modified systems, particularly at higher concentrations (86–114 g/L), produced significantly thicker filter cakes (0.09 ± 0.01) compared to the control (0.06 ± 0.01). This observation suggests that BCF enhances rapid pore plugging and facilitates early filter cake formation.

To quantitatively evaluate the sealing efficiency of the formed filter cakes, permeability was estimated using Darcy's law for static filtration. The calculated permeabilities are presented in Table 9. The lowest permeability values were recorded at 29 g/L and 57 g/L BCF concentrations (0.071 and 0.078 mD, respectively), indicating the formation of tighter and more effective filter cakes compared to the control (0.085 mD). Although higher BCF loadings (86–114 g/L) produced thicker cakes, they resulted in slightly higher permeability. Overall, the addition of BCF at optimal concentrations improved the filter cake quality by reducing its permeability, which correlates well with the observed reduction in early-stage filtrate invasion.

Table 9
Estimated filter cake permeability of the formulated muds.

Mud Sample	BCF Concentration (g/L)	Estimated Permeability (mD)
Control (NaOH)	0	0.085
BCF-29	29	0.071
BCF-57	57	0.078
BCF-86	86	0.112
BCF-114	114	0.110

The improved filtration behavior is attributed to the fibrous and carbonaceous nature of BCF, which promotes effective pore bridging and the development of a dense, low-permeability filter cake. With increasing filtration time, enhanced particle packing and interlocking within the cake structure further restrict filtrate invasion, resulting in improved long-term fluid loss control. Conventional filtration control additives such as polyanionic cellulose (PAC) and starch primarily reduce fluid loss through the formation of thin, low-permeability polymeric films on the wellbore wall [53].

Despite these difference in filtration mechanisms, the observed reduction in filtrate volume and formation of compact filter cakes in BCF-modified systems suggest comparable filtration performance. This indicates that BCF may serve as a complementary or alternative additive, particularly in formulations requiring both structural reinforcement and filtration control.

3.9. Mud cake thickness

Fig. 13 shows the mud cake thickness of various mud samples, each with different amounts of BCF. The control sample had a mud cake thickness of about 0.06 ± 0.01 in., which falls within the acceptable range for conventional water-based drilling fluids. After adding the BCF additive, BCF-29 had a mud cake thickness of 0.05 ± 0.008, while BCF-57 recorded a thickness of 0.06 ± 0.0008, similar to the control value, indicating a balanced contribution of BCF to filter cake formation without excessive buildup. However, increasing BCF concentrations further caused noticeable thickening of the mud cake, as BCF-86 and BCF-114 showed higher thicknesses of approximately 0.09 in., reflecting increased solids buildup at higher fiber loadings.

Statistical comparisons against the control (Table 10). Indicated that

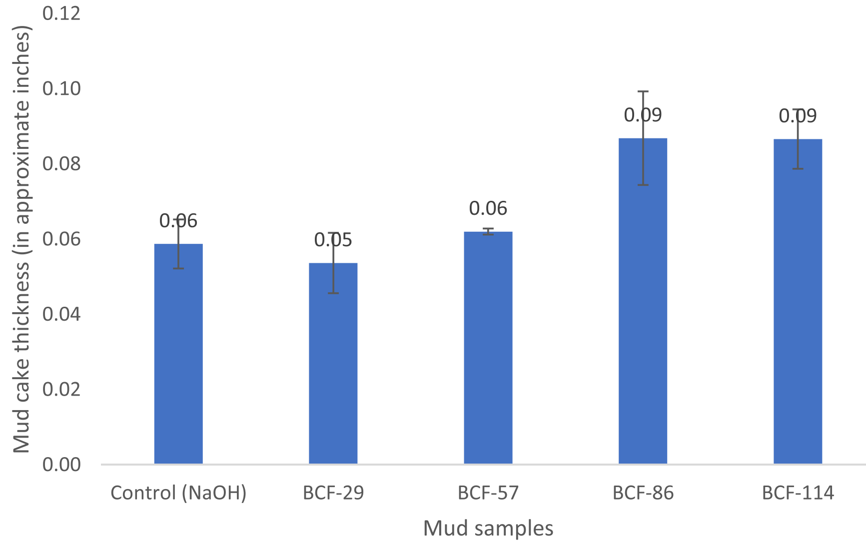

Fig. 13. Variation of filter cake thickness for control and BCF-modified drilling fluids after API filtration tests. Values are reported as mean ± standard deviation (n = 3), with statistical comparison performed using Welch's *t*-test (α = 0.05).

Table 10
Effect of BCF concentration on mud cake thickness and statistical significance relative to control.

Sample	BCF (g/L)	Mud Cake Thickness (inches)	Significance vs Control (Welch's *t*-test)
Control (NaOH)	0	0.06 ± 0.01	-
BCF-29	29	0.05 ± 0.008	p > 0.05 (ns)
BCF-57	57	0.06 ± 0.0008	p > 0.05 (ns)
BCF-86	86	0.09 ± 0.012	p < 0.05*
BCF-114	114	0.09 ± 0.007	p < 0.05*

Note
ns = not significant (p > 0.05).
* p < 0.05.

BCF-29 and BCF-57 showed no statistically significant difference from the control ($p > 0.05$), while BCF-86 and BCF-114 produced significantly thicker mud cakes than the control ($p < 0.05$). Differences among the BCF samples themselves were not statistically significant ($p > 0.05$), indicating that fiber concentration has a modest but clear effect on cake thickness within the tested range.

The observed increase in mud cake thickness at elevated BCF concentrations can be attributed to the fibrous nature of the additive, which promotes particle interlocking and structural buildup within the filter cake matrix. While thicker cakes can enhance wellbore sealing and reduce deep filtrate invasion, excessively thick mud cakes may increase the risk of differential sticking if not properly controlled.

These findings suggest that BCF is a bio-based additive that can enhance drilling fluid efficiency through both structural and chemical methods. More studies are needed under high-pressure, high-temperature conditions and with detailed compositional analysis to confirm its use in field operations.

Although physicochemical characterization was performed, a comprehensive analysis of ash composition was not conducted. The study also did not examine long-term stability, environmental impact, or directly compare results with common additives like PAC or starch. These aspects require further investigation to confirm their applicability in the field.

4. Conclusion

This study demonstrates that BCF is an effective multifunctional additive for water-based drilling fluids, with performance strongly governed by its physicochemical characteristics. The size distribution showed a finely divided material, with average particle sizes of 1727 nm. This characteristic can be advantageous for effective filtration control.

The SEM images revealed a highly porous, fibrous morphology that promotes mechanical interlocking and efficient pore bridging, facilitating the formation of a compact, low-permeability filter cake. It is noted that the rough surface morphology observed in BCF results from the calcination process, which alters the surface structure.

The FTIR spectra confirm the components reported in the coconut fiber literature and also show the degradation of hemicellulose structures during burning. The compositional insights from EDS further indicate the presence of inorganic constituents capable of contributing to mild alkalinity, thereby supporting pH stabilization. Thermogravimetric analyses investigated the application of BCF, and it was found that the material presents thermal stability at low to moderate temperatures.

Rheological evaluation showed that low to moderate BCF concentrations (29–57 g/L) produced the most favorable performance, characterized by a substantial reduction in plastic and apparent viscosity alongside the development of a robust yield point. resulting in improved flow efficiency and enhanced cuttings transport. In contrast, higher BCF concentrations (86–114 g/L) resulted in excessive thinning, highlighting the importance of dosage optimization. Gel strength measurements further confirmed that BCF enhances structural integrity during static conditions without inducing overly rigid gels that could impede circulation restart. Filtration tests indicated that the sample modified with BCF exhibited reduced early-stage filtrate invasion and formed thin, compact filter cakes at optimal concentrations, suggesting improved wellbore sealing and reduced formation damage potential. The observed pH moderation, from strongly alkaline values in the NaOH-based control to near-neutral levels (~8.0) across all BCF-containing samples, further highlights the additive's chemical stability. Lastly, BCF shows strong potential for field application as a supplementary additive in water-based drilling fluids, particularly for improving hole cleaning, filtration control, and pH stability. Its performance suggests suitability for conventional drilling operations.

5. Future studies

While the laboratory-scale performance of BCF as a drilling fluid additive is promising, more studies will be required to advance its application toward field-scale deployment. Therefore, future studies should give top priority to high-pressure, high-temperature (HPHT) testing to determine the thermal stability, rheological resilience, and filtration performance of BCF-modified fluids under practical downhole conditions.

Further research on the compatibility of BCF with conventional drilling fluid components, including bentonite, polymers, shale inhibitors, lubricants, and weighting agents, is needed to ensure stable performance in complex mud systems. Surface modification or controlled thermal activation of BCF can also be investigated to enhance its yield-point contribution while mitigating excessive thinning at higher dosages.

Future studies should also include SEM characterization of filter cake morphology to directly visualize particle packing, pore bridging, and the structural evolution of BCF-modified mud systems during filtration.

Advanced interfacial and microstructural analyses, including zeta potential measurements, rheo-optical studies, and dynamic filtration visualization, will be beneficial in elucidating the mechanisms controlling particle interactions, gel development, and filter cake formation.

From a sustainability perspective, life-cycle assessment and techno-economic analysis are recommended for future studies to quantify the environmental and cost advantages of BCF relative to conventional chemical additives.

CRediT authorship contribution statement

Kevin Igwilo: Formal analysis, Data curation. **Jeffrey Oseh:** Methodology, Investigation, Data curation. **Stephen Udeagbara:** Writing – review & editing, Writing – original draft. **Ifeanyi Oguamah:** Methodology, Investigation, Formal analysis, Conceptualization.

Declaration of Generative AI and AI-assisted technologies in the writing process

The authors hereby disclose that Generative AI and AI-assisted technologies, namely ChatGPT and Grammarly, were used solely to assist with language refinement and sentence structure. After using these tools, the authors reviewed and edited the manuscript accordingly.

Conflict of Interest

On behalf of all authors, the corresponding author states that there is no conflict of interest.

Declaration of Competing Interest

The authors declare that they have no known competing financial interests or personal relationships that could have appeared to influence the work reported in this paper.

Data Availability

The datasets generated and analyzed during the current study are available from the corresponding author on reasonable request.

References

[1] Chapter II – drilling fluids, in: J.K. Fink (Ed.), Water-Based Chemicals and Technology for Drilling, Completion, and Workover Fluids, Gulf Professional Publishing, 2015, pp. 5–114, https://doi.org/10.1016/B978-0-12-802505-5.00002-0.

[2] A.N. Okon, J.U. Akpabio, K.W. Tugwell, Evaluating the locally sourced materials as fluid loss control additives in water-based drilling fluid, Heliyon 6 (5) (2020) e04091, https://doi.org/10.1016/j.heliyon.2020.e04091.

[3] A. Mohamed, S. Salehi, R. Ahmed, Significance and complications of drilling fluid rheology in geothermal drilling: a review, Geothermics 93 (2021) 102066, https://doi.org/10.1016/j.geothermics.2021.102066.

[4] A. Rafieefar, F. Sharif, A. Hashemi, A.M. Bazargan, Rheological behavior and filtration of water-based drilling fluids containing graphene oxide: experimental measurement, mechanistic understanding, and modeling, ACS Omega 6 (44) (2021) 29905–29920, https://doi.org/10.1021/acsomega.1c04398.

[5] A. Esfandyari Bayat, S. Harati, H. Kolivandi, Evaluation of rheological and filtration properties of a polymeric water-based drilling mud in presence of nano additives at various temperatures, Colloids Surf. A: Physicochem. Eng. Asp. 627 (2021) 127128, https://doi.org/10.1016/j.colsurfa.2021.127128.

[6] O.E. Agwu, J.U. Akpabio, M.E. Ekpenyong, U.G. Inyang, D.E. Asuquo, I.J. Eyoh, O. S. Adeoye, A critical review of drilling mud rheological models, J. Pet. Sci. Eng. 203 (2021) 108659, https://doi.org/10.1016/j.petrol.2021.108659.

[7] Y. Assef, D. Arab, P. Pourafshary, Application of nanofluid to control fines migration to improve the performance of low salinity water flooding and alkaline flooding, J. Pet. Sci. Eng. 124 (2014) 331–340, https://doi.org/10.1016/j.petrol.2014.09.023.

[8] M.H. Rasool, A. Zamir, K.A. Elraies, M. Ahmad, M. Ayoub, M.A. Abbas, I. Ali, Rheological characterization of potassium carbonate deep eutectic solvent (DES) based drilling mud, J. Pet. Explor. Prod. Technol. 12 (7) (2022) 1785–1795, https://doi.org/10.1007/s13202-021-01328-6.

[9] Y. Li, W. Cao, W. Hu, M. Wu, Identification of downhole conditions in geological drilling processes based on quantitative trends and expert rules, Neural Comput. Appl. 35 (17) (2023) 12297–12306, https://doi.org/10.1007/s00521-021-05759-4.

[10] H. Gamal, S. Elkatatny, S. Basfar, A. Al-Majed, Effect of pH on rheological and filtration properties of water-based drilling fluid based on bentonite, Sustainability 11 (23) (2019), https://doi.org/10.3390/su11236714.

[11] A.T.T. Al-Hameedi, H.H. Alkinani, S. Dunn-Norman, M.A. Al-Alwani, A. F. Alshammari, H.W. Albazzaz, M.M. Alkhamis, N.F. Alashwak, R.A. Mutar, Insights into the application of new eco-friendly drilling fluid additive to improve the fluid properties in water-based drilling fluid systems, J. Pet. Sci. Eng. 183 (2019) 106424, https://doi.org/10.1016/j.petrol.2019.106424.

[12] S. Zheng, Z. Huang, A. Yao, Research on the effect of drilling fluid's pH value on the coal's wettability, J. Pet. Explor. Prod. Technol. 8 (3) (2018) 849–853, https://doi.org/10.1007/s13202-017-0374-7.

[13] M.-C. Li, Q. Wu, K. Song, A.D. French, C. Mei, T. Lei, PH-responsive water-based drilling fluids containing bentonite and chitin nanocrystals, ACS Sustain. Chem. Eng. 6 (3) (2018) 3783–3795, https://doi.org/10.1021/acssuschemeng.7b04156.

[14] S. Yahya, K.E. Kee, M.J.M. Puad, M.C. Ismail, Evaluation on steel corrosion in water-based drilling fluids: Inhibitors and scale involvement, J. Pet. Sci. Eng. 211 (2022) 110127, https://doi.org/10.1016/j.petrol.2022.110127.

[15] I. Ali, M. Ahmad, T.A.-A. Ganat, Experimental study on water-based mud: investigate rheological and filtration properties using cupressus cones powder, J. Pet. Explor. Prod. Technol. 12 (10) (2022) 2699–2709, https://doi.org/10.1007/s13202-022-01471-8.

[16] B. Borah, B.M. Das, A review on applications of bio-products employed in drilling fluids to minimize environmental footprint, Environ. Chall. 6 (2022) 100411, https://doi.org/10.1016/j.envc.2021.100411.

[17] K.C. Igwilo, I. Oguamah, S.C. George, N. Uwaezuoke, U. Obubike, Evaluation of the suitability of Pleurotus as a fluid loss control agent using the chemical structural properties approach, Sci. Afr. 19 (2023) e01468, https://doi.org/10.1016/j.sciaf.2022.e01468.

[18] H.H. Alkinani, A.T. Al-Hameedi, R.E. Flori, Experimental investigation of a new bio enhancer drilling fluid additive: Palm tree leaves powder (PTLP), J. Pet. Explor. Prod. Technol. 9 (2019) 2753–2763, https://doi.org/10.1007/s13202-019-00766-7.

[19] A.T. Al-Hameedi, H.H. Alkinani, R.E. Flori, S. Dunn-Norman, Utilizing a new eco friendly drilling mud additive generated from wastes to minimize the use of conventional chemical additives, J. Pet. Explor. Prod. Technol. 10 (2) (2020) 1001–1013, https://doi.org/10.1007/s13202-020-00974-6.

[20] M.A.I. Shuvo, M.Z.B. Sultan, A.R. Ferdous, Applicability of sawdust as a green additive to improve the rheological and filtration properties of water based drilling fluid: an experimental investigation, J. Pet. Explor. Prod. Technol. 14 (1) (2023) 303–315, https://doi.org/10.1007/s13202-023-01706-2.

[21] G. Zhou, Z. Qiu, H. Zhong, X. Zhao, X. Kong, Study of environmentally friendly wild jujube pit powder as a water-based drilling fluid additive, ACS Omega 6 (2) (2021) 1436–1444, https://doi.org/10.1021/acsomega.0c05108 (219, 111234).

[22] M. Murtaza, Z. Tariq, X. Zhou, D. Al-Shehri, M. Mahmoud, M. Kamal, Okra as an environment-friendly fluid loss control additive for drilling fluids: experimental & modeling studies, J. Pet. Sci. Eng. 204 (2021) 108743, https://doi.org/10.1016/J.PETROL.2021.108743.

[23] O.I. Oladipo, F. Faraji, H. Habibi, M. Abdalqadir, J.A. Ali, P.L. Chong, Feasibility study of biodegradable vegetable peels as sustainable fluid loss additives in water-based drilling fluids, J 8 (1) (2025), https://doi.org/10.3390/j8010010.

[24] M.A. Khan, K. Lv, J. Sun, F. Liu, H. Shen, Y. Ding, A.A. Noor, S.M. Lalji, C. Liu, M.-C. Li, Enhanced filtration performance of cellulose nanofiber/bentonite water-based drilling fluids with temperature- and salt-resistant polymers for extreme conditions, SPE J. 30 (09) (2025) 5327–5349, https://doi.org/10.2118/228402-PA.

[25] M.A. Khan, M.-C. Li, K. Lv, J. Sun, C. Liu, X. Liu, H. Shen, L. Dai, S.M. Lalji, Cellulose derivatives as environmentally-friendly additives in water-based drilling fluids: a review, Carbohydr. Polym. 342 (2024) 122355, https://doi.org/10.1016/j.carbpol.2024.122355.

[26] M.A. Khan, K. Lv, J. Sun, H. Shen, Y. Zhang, A.A. Noor, S.M. Lalji, C. Liu, M.-C. Li, Influence of salt and temperature on the rheological and filtration properties of cellulose Nanofiber/bentonite water-based drilling fluids, Geoenergy Sci. Eng. 244 (2025) 213524, https://doi.org/10.1016/j.geoen.2024.213524.

[27] M.T. Safian, B.R. Pandian, N.E.A. Kahar, M.N.M. Ibrahim, Mechanical exfoliation of coconut husk into bio-based graphene for sustainable drilling mud: a Taguchi–GRA study, Carbon Lett. (2025), https://doi.org/10.1007/s42823-025-00938-y.

[28] M.T. Al-saba, K.W. Amadi, K.O. Al-Hadramy, M.F. Dushaishi, A. Al-Hameedi, H. Alkinani, Experimental Investigation of Bio-degradable Environmentally Friendly Drilling Fluid Additives Generated from Waste (D021S007R003), 2018 (⟨https://doi.org/10.2118/190655-MS⟩).

[29] M. Idress, M.L. Hasan, Investigation of different environmentally friendly waste materials as lost circulation control additives in water-based drilling fluids, J. Pet. Explor. Prod. Technol. 10 (2020) 2843–2856, https://doi.org/10.1007/s13202-019-00752-z.

[30] J.O. Oseh, M.N.A.M. Norddin, A. Kerunwa, I. Ismail, H.M. Warsame, J. R. Gbonhinbor, E.N. Ngouangna, S.I. Okwaraku, I.M. Onyejekwe, I.A. Oguamah, M.N. Yahya, A. Agi, Improvement of Static and Dynamic Sag Performance of Water-Based Drilling Mud Using Combined Nano-Barite and Nano-Ilmenite Particles (D031S024R002), 2025 (⟨https://doi.org/10.2118/228676-MS⟩).

[31] M.I. Magzoub, S. Salehi, I.A. Hussein, M.S. Nasser, Investigation of filter cake evolution in carbonate formation using polymer-based drilling fluid, ACS Omega 6 (9) (2021) 6231–6239, https://doi.org/10.1021/acsomega.0c05802.

[32] S. Mahalakshmi, R. Jayaseelan, G. Pandulu, Microstructural and mechanical performance of coconut shell biochar – modified asphalt for sustainable pavement applications, Materials 11 (2026) 101595, https://doi.org/10.1016/j.nxmate.2026.101595.

[33] K.M.F. Hasan, P.G. Horváth, M. Bak, T. Alpár, A state-of-the-art review on coir fibre-reinforced biocomposites, RSC Adv. 11 (18) (2021) 10548–10571, https://doi.org/10.1039/D1RA00231G.

[34] F.L. Morbeck, R.C.C. Lelis, M.V.E. Schueler, W.A. Santos, D.A. Sampaio, B.C. da Silva, R. de M. Morais, G.M. Santana, Extraction and evaluation of tannin from green coconut mesocarp, Matéria 24 (3) (2019) e12433, https://doi.org/10.1590/S1517-707620190003.0748.

[35] Rengasamy Ragupathi Raja Kannan, Rajasekaran Arumugam, Perumal Anantharaman, Fourier transform infrared spectroscopy analysis of seagrass polyphenols, Curr. Bioact. Compd. 7 (2) (2011) 118–125, https://doi.org/10.2174/157340711796011142.

[36] A. Koochakzaei, M. Sabaghian, Tannin characterization and sourcing in historical leathers through FTIR spectroscopy and PCA analysis, Collagen Leather 5 (1) (2023) 21, https://doi.org/10.1186/s42825-023-00128-4.

[37] C.L. Mendoza Martinez, E. Sermyagina, J. Saari, M. Silva de Jesus, M. Cardoso, G. Matheus de Almeida, E. Vakkilainen, Hydrothermal carbonization of lignocellulosic agro-forest based biomass residues, Biomass Bioenergy 147 (2021) 106004, https://doi.org/10.1016/j.biombioe.2021.106004.

[38] S. Marchuk, A. Marchuk, Effect of applied potassium concentration on clay dispersion, hydraulic conductivity, pore structure and mineralogy of two contrasting Australian soils, Soil Tillage Res. 182 (2018) 35–44, https://doi.org/10.1016/j.still.2018.04.016.

[39] Y.A. Abdulhameed, J.A. Ali, L.A. Abdulkareem, Assessment of KCl inhibition efficiency in water-based drilling fluids: a formation-responsive approach for shale stability, Ind. Eng. Chem. Res. 64 (45) (2025) 21523–21539, https://doi.org/10.1021/acs.iecr.5c03075.

[40] W. Zheng, S. Wang, L. Bai, F. Xue, Adaptability of evaluation methods for the inhibitory effect of potassium-based inhibitors in drilling fluids, Results Chem. 20 (2026) 102990, https://doi.org/10.1016/j.rechem.2025.102990.

[41] B.R. Freitas, J.D.O. Braga, M.P. Orlandi, B.P. da Silva, I.V. Aoki, V. de F.C. Lins, F. Cotting, Characterization of coir fibre powder (Cocos nucifera L.) as an environmentally friendly inhibitor pigment for organic coatings, J. Mater. Res. Technol. 19 (2022) 1332–1342, https://doi.org/10.1016/j.jmrt.2022.05.098.

[42] Y. Nagaashi, T. Omura, M. Kiuchi, A.M. Nakamura, K. Wada, S. Hasegawa, Laboratory experiments on agglomeration of particles in a granular stream, Prog. Earth Planet. Sci. 5 (1) (2018) 52, https://doi.org/10.1186/s40645-018-0205-6.

[43] A. Bera, S. Kumar, A. Mandal, Temperature-dependent phase behavior, particle size, and conductivity of middle-phase microemulsions stabilized by ethoxylated nonionic surfactants, J. Chem. Eng. Data 57 (12) (2012) 3617–3623, https://doi.org/10.1021/je300845q.

[44] B.S. Aadnøy, R. Looyeh, Chapter 10—drilling design and selection of optimal mud weight, in: B.S. Aadnøy, R. Looyeh (Eds.), Petroleum Rock Mechanics, Second Edition, Gulf Professional Publishing, 2019, pp. 165–181, https://doi.org/10.1016/B978-0-12-815903-3.00010-8.

[45] Okrajni, S.S., Azar, J.J. (1C.E.), The Effects of Mud Rheology on Annular Hole Cleaning in Directional Wells, SPE (Society of Petroleum Engineers) Drill. Eng., United States, 1:4. https://doi.org/10.2118/14178-PA.

[46] R. Gautam, M. Sahai, S. Kumar, Recent advances in application of nanomaterials as additives for drilling fluids, Energy Sources Part A: Recovery Util. Environ. Eff. 47 (1) (2025) 3496–3519, https://doi.org/10.1080/15567036.2020.1855273.

[47] H. Al-Ziyadi, A. Verma, Investigating the synergistic effects of coconut coir fiber and xanthan gum on the rheology and filtration loss of water-based drilling fluids, Pet. Sci. Technol. (2024) 1–17, https://doi.org/10.1080/10916466.2024.2445696.

[48] A.Ya Malkin, S.R. Derkach, V.G. Kulichikhin, Rheology of gels and yielding liquids, Gels 9 (9) (2023) 715, https://doi.org/10.3390/gels9090715.

[49] M.R. Islam, M.E. Hossain, Chapter 2—state-of-the-art of drilling, in: M.R. Islam, M. E. Hossain (Eds.), Drilling Engineering, Gulf Professional Publishing, 2021, pp. 17–178, https://doi.org/10.1016/B978-0-12-820193-0.00002-2.

[50] A.A. Awoyale, D. Lokhat, P. Okete, Investigation of the effects of pretreatment on the elemental composition of ash derived from selected Nigerian lignocellulosic biomass, Sci. Rep. 11 (1) (2021) 21313, https://doi.org/10.1038/s41598-021-00672-1.

[51] G. Ondrasek, M. Zovko, F. Kranjčec, R. Savić, D. Romić, Z. Rengel, Wood biomass fly ash ameliorates acidic, low-nutrient hydromorphic soil & reduces metal accumulation in maize, J. Clean. Prod. 283 (2021) 124650, https://doi.org/10.1016/j.jclepro.2020.124650.

[52] I. Ali, M. Ahmad, Investigation of rheological and filtration behavior of tapioca starch in nondamaging water-based muds, in: AIP Conference Proceedings, 2610, 2022 030011, https://doi.org/10.1063/5.0100106.

[53] F. You, Y. Zheng, X. Gong, Filtration control properties of four native starches in water-based drilling fluids, Int. J. Biol. Macromol. 283 (2024) 137580, https://doi.org/10.1016/j.ijbiomac.2024.137580.